Status and Strategy of CLAM Steel for Fusion Application in China

Qunying Huang, FDS Team

Key Laboratory of Neutronics and Radiation Safety, Institute of Nuclear Energy Safety Technology, Chinese Academy of Sciences, Hefei, Anhui, 230031, China

E−mail: qunying.huang@fds.org.cn

Abstract: A program for China Low Activation Martensitic (CLAM), since 2001, aims to satisfy the material requirements of test blanket module (TBM) for ITER, China fusion engineering test reactor (CFETR) and fusion demonstration reactor (C-DEMO) in China. It has been undertaking by INEST (Institute of Nuclear Energy Safety Technology, Chinese Academy of Science) under wide domestic and international collaborations. Recent years CLAM steel has been chosen as the primary structural material of CN helium cooled ceramic breeder (HCCB) TBM for ITER. To license a pressurized nuclear equipment e.g. the ITER-TBM and the blanket for DEMO, it needs to present the design and safety analyses with sufficient data such as the consolidated materials data, design limits and qualified fabrication procedures specifications etc. to the Regulator (ESP/ESPN) and the Agreed Notified Body (ANB) of France or China's Nuclear Safety Agency. A lot of work and efforts are being devoted on the R&D of CLAM steel to its final successful application in the fusion systems. Its properties database basically meets the requirement of the qualification for ITER-TBM. The status and strategy of the CLAM steel project are reviewed in this paper.

1. A brief introduction to CLAM steel

Reduced activation ferritic/martensitic (RAFM) steel is considered as one of the most promising candidates for structure materials of fusion reactors due to its high strength, good heat conductivity, resistance to irradiation and low activation features [1-4]. For example, RAFM steel is chosen as the structural materials for all the six International Thermonuclear Experimental Reactor (ITER) test blanket modules (TBM). The China low activation martensitic (CLAM) steel is developed leading by the Institute of Nuclear Energy Safety Technology (INEST), Chinese Academy of Sciences (CAS) with participation of more than thirty domestic and overseas research units [5-7].

It has been chosen as the structural material in the design of FDS series PbLi blankets for fusion reactors and China fusion engineering test reactor (CFETR) blanket in China [8-10]. Especially, it has been chosen as the primary candidate structural material for Chinese helium cooled ceramic breeder (HCCB) TBM for ITER.

Since the TBMs will be tested in ITER, the properties of CLAM steel have to be evaluated and assessed based on the French regulations on pressure vessel equipment, probably in its nuclear extension, as well as high standards of quality assurance required for reliable and safe operation of ITER. A lot of efforts are being devoted on the development of CLAM steel in material fabrication processes [11], material property evaluation (including mechanical properties [12], corrosion [13], irradiation [14-15] and joining [16-17] etc.) and the establishment of a material database for its successful application in CN ITER-TBM. The status and strategy of these activities for CLAM steel are reviewed in this paper.

2. Newly prepared 6.4-ton CLAM steel and its properties

2.1 Chemical composition design & Fabrication process control

Alloy chemistry refinement has been explored for RAFM steels, leading to the evolution of Eurofer97-1 to Eurofer97-2 and F82H-IEA to F82H-mod and F82H-BA. More dramatic alloy composition adjustment of RAFM steels has also been pursued. For instance, increasing the percentage of Ta (~ 0.2 wt %) exhibited some improvements in both the impact properties and creep resistance despite the negligible influence on yield strength [18]. According to this result, one industrial scale ingot of 6.4 tons, named HEAT 1506, was fabricated with vacuum induction melting (VIM) and vacuum arc remelting (VAR). Two types of plates, with the sizes of 7600 mm×1550 mm×15 mm and 2100 mm× 1500 mm×52 mm, were fabricated. The heat treatment is normalizing at 1000 °C for 40 min and then cooling in water and tempering at 740 °C for 90 min and then cooling in air.

The chemical compositions of the product are listed in Table 1. According to the French code RCC-MRx, the analysis on the structure and the grain size was carried out. The microstructure of as-received CLAM steel was tempered martensite. The delta ferrite content was less than 3%. The presence of primary carbides was not found. The austenitic grain size index was measured to be greater than 8. The non-metallic inclusion rate was less than 1 for type A, B, C and D inclusions.

Table 1. Chemical compositions of 6.4-ton CLAM steel (wt %).

	Cr	W	Ta	V	C	Si	Mn	P	S	O	N	Fe
HEAT 1506	9.11	1.52	0.20	0.19	0.12	0.03	0.41	0.003	0.003	0.001	0.002	Bal.

2.2 Mechanical properties

2.2.1. Effect of refining processes on tensile and Charpy impact properties

The influence of smelting processes on mechanical properties of CLAM steel was investigated. As shown in Table 2 [7], the combination process of VIM, electro-slag remelting (ESR) and VAR could further decrease the total amount of impurity elements including O, N, S and P etc. It can help to obtain more uniform distribution of Ta in the matrix, which leads to higher strength and lower ductile brittle transition temperature (DBTT) as shown in Figs. 1 and 2.

Table 2. Four refining processes and impurity contents of CLAM steels [7].

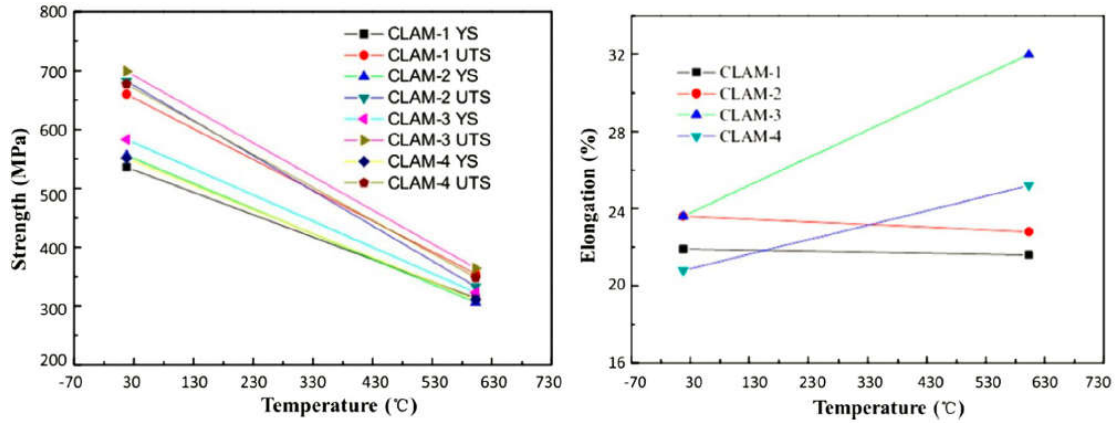| Ingot No.	Refining process	Sum of impurity contents of O, N, S, P (ppm)
CLAM-1	VIM	205
CLAM-2	VIM + ESR	228
CLAM-3	VIM + ESR + VAR	133
CLAM-4	VIM + VAR	205

Fig. 1. Effect of different refining processes on tensile properties [7].
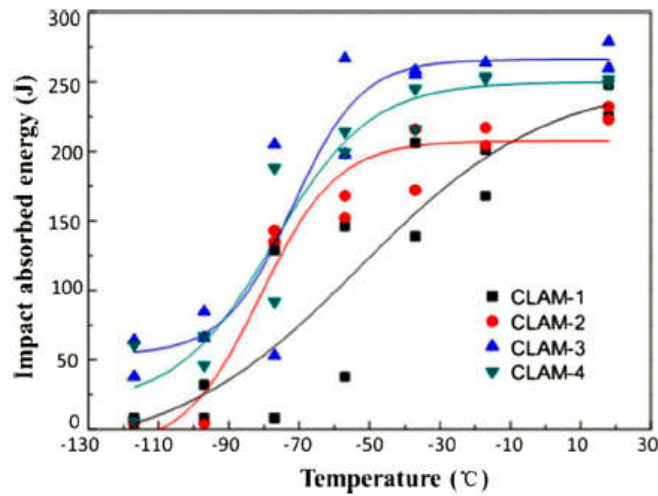

Fig. 2. Effect of different refining processes on Charpy impact absorption energy [7].

2.2.2. Fatigue properties

The low cycle fatigue (LCF) behavior of CLAM steel has been studied using a constant strain rate of 8×10^{-3}/s with the strain amplitudes ranging from 0.3% to 0.8% at 450 °C and 550 °C. Cyclic stress response showed a gradual softening until complete failure. The fatigue life decreased with increasing test temperature, and the effect of temperature on fatigue life was more pronounced at lower strain amplitudes. At a given strain amplitude, the steel exhibited rapid initial softening followed by gradual softening until the onset of the final stress drop, which was accompanied by the initiation and propagation of a fatigue crack. The same trends were noticed at all test temperatures and strain amplitudes, as shown in Fig. 3.
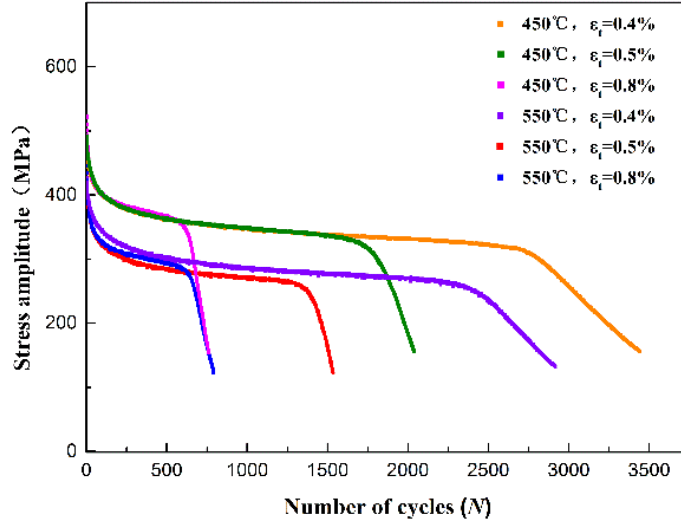
Fig. 3. Cyclic stress response curves of CLAM steel [19].

The change of tensile stress magnitude induced by cyclic loading was evaluated by comparing the monotonic and cyclic stress–strain curves [20]. The cyclic stress-strain curve was determined by connecting the tips of the stable hysteresis loops of the fatigue tested specimens for different strain amplitudes and temperatures as shown in Fig. 4. Comparing the monotonic and cyclic stress-strain curves, it showed that cyclic loading resulted in lower strength at both test temperatures.

450°C   550°C
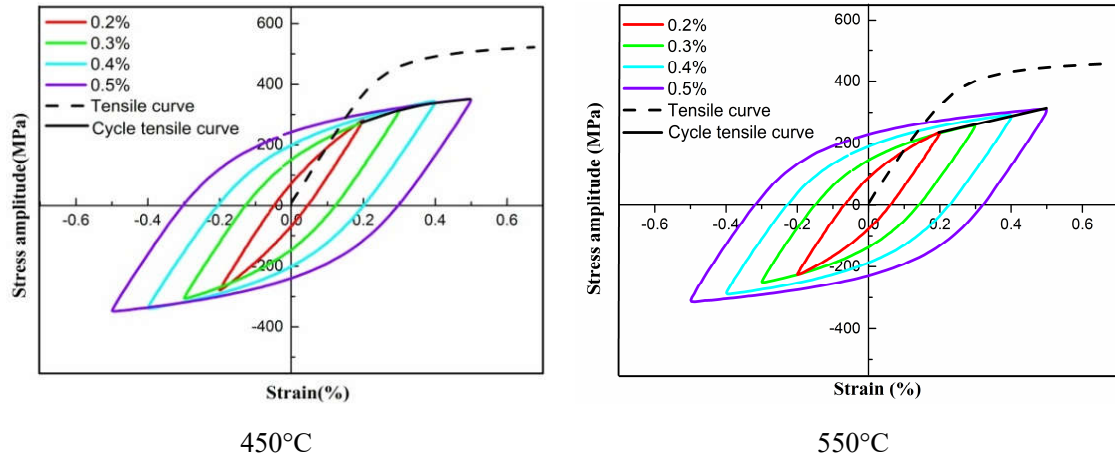
Fig. 4. Comparison between monotonic and cyclic stress–strain behaviors [19].

In order to properly analyze the stress–strain response under cyclic loading, a Ramberg-Osgood type equation was used, which is defined based on the cyclic strength coefficient (K) and strain hardening exponent (m) [20]:

$$\overline{\Delta\varepsilon_t}(\%) = 100 * \frac{2(1+\nu)}{3E}(\frac{\overline{\Delta\sigma}}{K})^{1/m} \tag{1}$$

Where $\overline{\Delta\varepsilon_t}$ is the total strain range, E is the Young's modulus at the test temperature (GPa), ν is the Poisson ratio, $\overline{\Delta\sigma}$ is the total stress range (MPa). The K (MPa) and m values obtained through applying the total strain and stress range in Fig. 5 to equation (1) are listed in Table 3. The stress at which the plastic extension is equal to 0.2% was used to represent the yield strength under cyclic loading, and the

cyclic yield strengths are 304 MPa and 263 MPa at 450 °C and 500 °C, respectively.

Table 3. Cyclic stress–strain parameters.

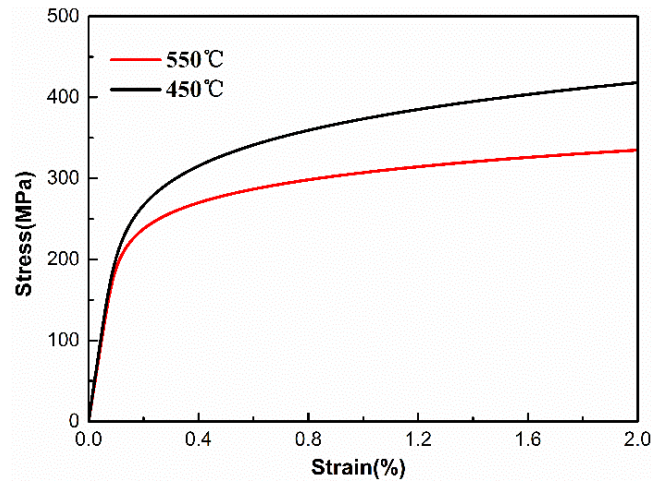| Temperature (°C)	K(MPa)	m
450	692.75	0.146
550	578.0	0.113

Fig. 5. Calculated cyclic stress–strain curves at 450 °C and 550 °C [19].

The microstructure evolution in CLAM specimens during the LCF tests was investigated, the subgrain size and dislocation densities of these samples are listed in Table 4. It is clear that dislocation densities decreased and subgrain size coarsened due to a coalescence of two or more neighboring subgrains. The subgrain size coarsening process was accelerated at higher test temperatures.

Table 4. Test results of subgrain sizes and dislocation densities.

Conditions of the sample	Base metal	550°C, $\Delta\varepsilon_t$=0.4%, 2711 cycles	450°C, $\Delta\varepsilon_t$=0.8%, 865 cycles	550°C, $\Delta\varepsilon_t$=0.8%, 654 cycles
Subgrain size (μm)	0.57	0.71	0.62	0.85
Number of subgrains	212	230	242	235
Dislocation densities (m^{-2})	$2.6*10^{14}$	$0.6*10^{14}$	$1.1*10^{14}$	$0.4*10^{14}$
Number of subgrains	18	22	20	20

2.2.3. Fracture toughness

The fracture toughness is one of the important material parameters to evaluate the performance of structural materials under complex mechanical loads. The fracture tests for CLAM steel were carried out at room temperature with three compact tension specimens according to ASTM E1820-2011. From the J–R curve shown in Fig. 8, the fracture toughness JIC was 417.9 ± 6.8 kJ/m^2. The microstructure observation on crack surfaces showed that the fracture occurred in a typical ductile fracture mode.

The fracture toughness was calculated on the basis of the fractal dimension by the analysis of fracture surface under plane strain with the vertical section method and image analysis technique [21]. The calculated JIC was 454.59 kJ/m^2 as shown in Fig. 6. The relative error of JIC for the experimental and calculated results was 8.1%.
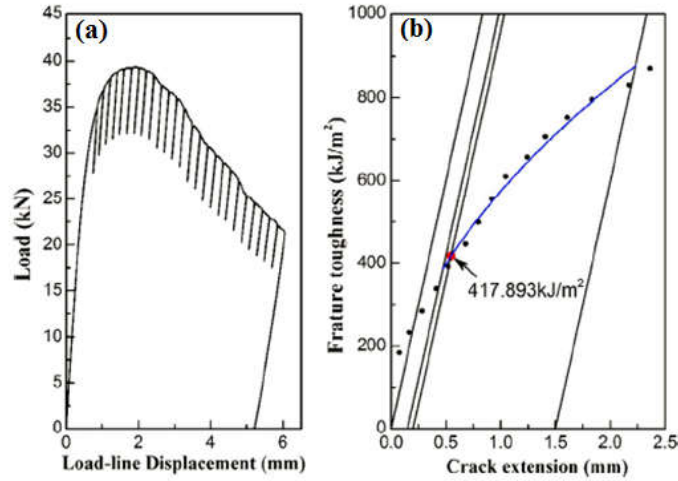

Fig. 6. Load and load-line displacement curve (a) and J–R curve (b).

2.3.4. Creep property

The creep resistance is one of the most important properties for the application of the RAFMs in fusion reactors under long-time loading at high temperature. The constant load creep tests of CLAM (HEAT 0912) were carried out at 500 °C, 550 °C and 600 °C, respectively, with stresses ranging from 150 MPa to 300 MPa [22]. The samples for creep testing were round with diameter 5 ± 0.02 mm and the gauge length was 50 ± 0.1 mm. As shown in Fig. 7, the creep curve exhibited three regimes i.e. primary, secondary and tertiary creep, which indicated a normal creep behavior. With the increase in test temperature from 550 °C to 600 °C, the stress exponent n varied from 19 to 15. The activation energy Q was ~676 kJ/mol at the temperature of 550-600 °C with the constant stress of 200 MPa. The fracture surfaces of specimens were examined by scanning electron microscopy (SEM). The fractographs indicated transgranular fracture under all the test conditions with the character of dimples owing to combination of micro-voids. Fig. 8 shows the microstructure of a CLAM specimen observed with transmission electron microscopy (TEM) after creep testing at 550 °C with a stress of 200 MPa for 1595 h. The diameter of $M_{23}C_6$ precipitates in the matrix increased from 100–150 nm to 200 nm during the long-time creep test. The long-time creep test for CLAM steel e.g. at 550 °C with stress of 150 MPa is underway.
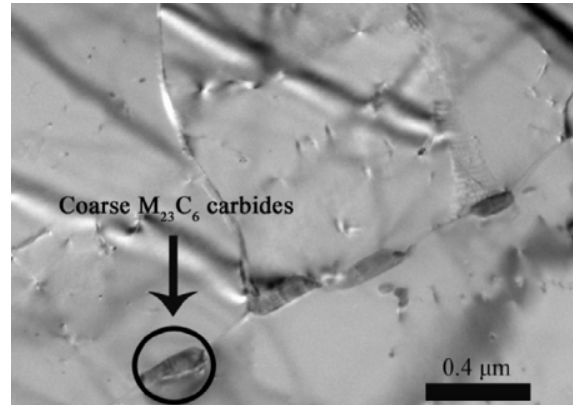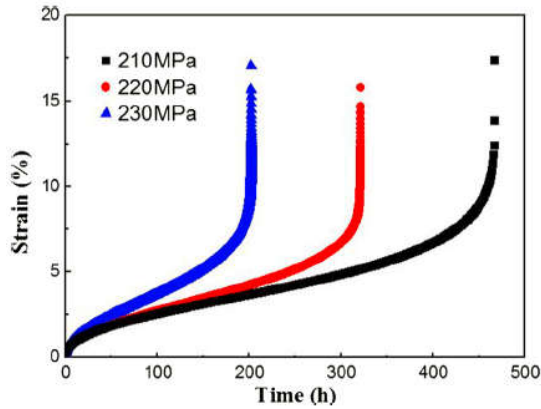
Fig. 7. Creep curves of CLAM steel at 550 °C [22]. Fig. 8. Coarse M₂₃C₆ carbides on subgrain Boundaries [22].

2.2.5. Thermal aging

Aging effect is another one of the key factors related to the design limit of RAFM steel, because thermal aging could cause significant change of microstructure and then the degradation of the mechanical properties. Investigation on the microstructure evolution and their impact on mechanical properties of CLAM steels was carried out in air at 600 °C and 650 °C for 1100 h, 3000 h and 5000 h, respectively [23]. The DBTT of the thermally-aged CLAM specimens increased to about -10 °C and -20 °C after 5000 h aging at 600 °C and 650 °C, respectively. During long-term thermal aging at 600 °C and 650 °C, the $M_{23}C_6$ carbides (60-200 nm) had a strong pinning effect on the migration of the subgrain boundaries while the fine MX carbonitrides (10-40 nm) had negligible effect on grain growth. The Laves-phase showed much slower growth kinetics at 650 °C than that at 600 °C. This indicated that the nose temperature of Laves-phase formation in the CLAM steel was probably lower than 650 °C. The results showed that Laves-phase had a small impact on the strength at the early stage of precipitation, but the formation of Laves-phase was detrimental to the impact toughness.

2.3 Irradiation tests

To promote the application process of CLAM steel, series of neutron irradiation experiments of CLAM steel have being carried out. The fission neutron irradiation experiments reached the dose of 2.98dpa, which is closed to the total dose level of ITER, in high flux engineering test reactor (HFETR) collaborated with Nuclear Power Institute of China (NPIC). The spallation neutron irradiation experiments were done with the dose up to 21 dpa, which is closed to the dose level of DEMO per year, in Swiss spallation neutron source (SINQ) collaborated with Paul Scherrer Institut (PSI) in Switzerland. Fig.9 shows the compared results of neutron irradiation properties of CLAM steel with Eurofer and F82H etc. at similar irradiation condition. These two types of irradiation experiments verified that the performance of CLAM steel after neutron irradiation were almost the same with that of F82H and Eurfer97 irradiated under similar irradiation condition with both fission and spallation neutron irradiation.
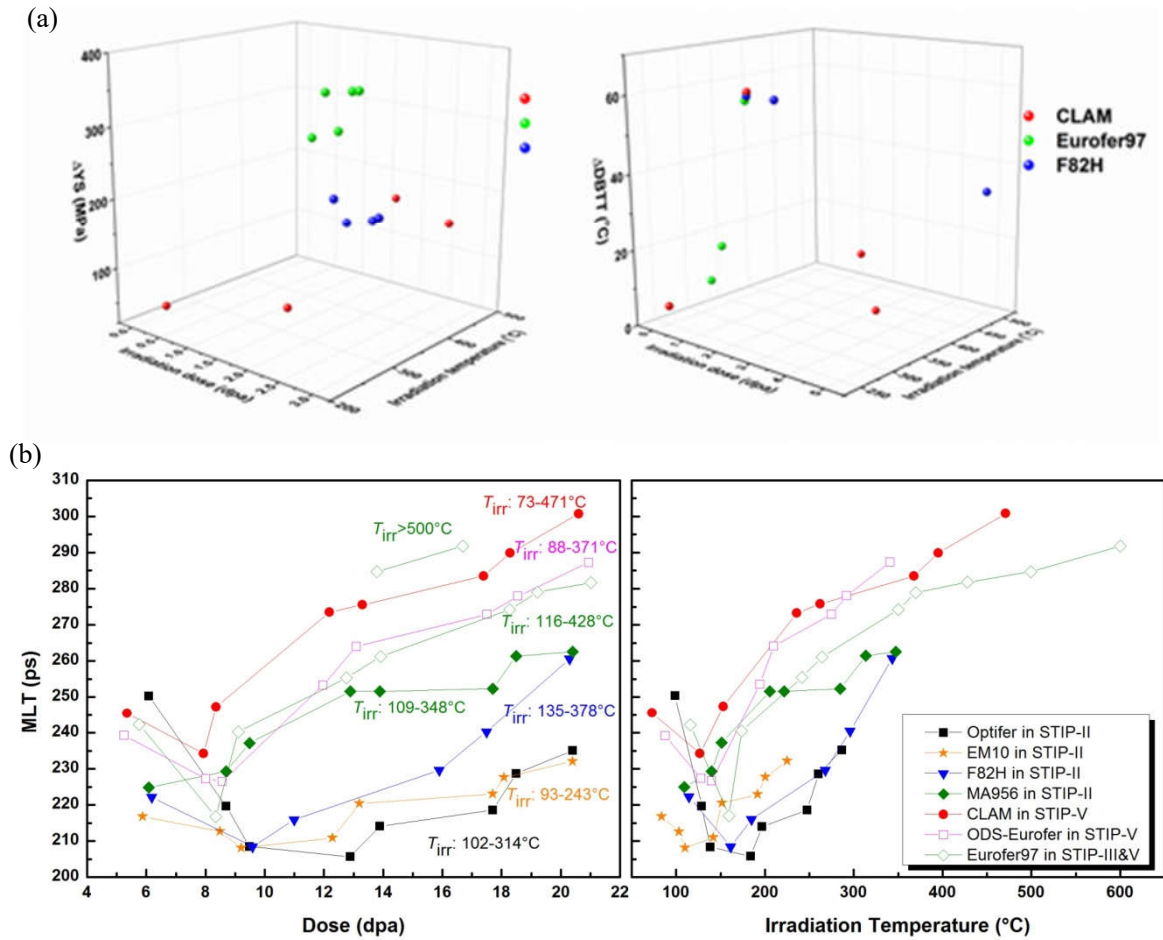
Fig. 9. Neutron irradiation properties of CLAM steel at ITER dose level (a) and dose level of DEMO per year (b).

Based on these experiences, full project on neutron irradiation performance evaluation of CLAM steel has been made according the requirement of fusion reactor engineering application. In the new project, physical and mechanical properties of CLAM steel irradiated up to ~100dpa at 300-500 °C in nuclear reactor will be tested following the detail requirement of RCC-MRx code. The neutron irradiation properties of CLAM steel, including specific heat, thermal resistivity, thermal conductivity, Poisson's ratio, creep, fatigue, fracture toughness, tensile, impact, as well as the welding technique, will be obtained with neutron irradiation dose of ~3 dpa and 50-100dpa gradually to meet the application permission at different step on the road map of ITER and fusion reactors in China.

At the same time, though a large number of neutron irradiation facilities have been proposed to evaluate the performance of structural materials for fusion reactor, such as HFETR, HFR, HFIR, SINQ, etc., it is at present not possible to reliably predict the degradation of materials exposed to fusion reactions for a long time with the available data. So a suitable fusion neutron irradiation apparatus and a method which can solve the equivalence of the results obtained using fission or spallation neutron with using fusion neutron have become an urgent issue to perform the evaluation of the material performance. The high intensity D-T fusion neutron generator (HINEG) under development in INEST with neutron energy of 14.1 MeV and neutron yield of ~10^{14} n/s, will be much more suitable for this purpose for CLAM steel's final application in fusion reactor. In addition, the multiscale modeling for atomic-scale to continuum-scale can be utilized to bridge the phenomena associated with irradiation damage effects

of materials in different neutron irradiation facilities.

2.4 Welding

It is a great challenge to fabricate the TBM with good quality due to its complex structures. A lot of efforts had being devoted on the weldability of CLAM steel with different welding technologies such as hot isostatic pressing (HIP) diffusion bonding, electron beam welding (EBW), tungsten inner gas (TIG) welding and laser beam welding (LBW). According to the Schaeffler constitution diagram, the composition of CLAM steel showed an obvious tendency to form δ-ferrite in the weld metal, which was detrimental to the impact toughness of the welded joints. Composition trimming of the filler wire compared to base metal has been conducted to depress the residual of δ-ferrite. The microstructure of multilayer butt-weld CLAM joint with modified filler wire under series of welding parameters was investigated. The area fraction of δ-ferrite in the center of weld metal and at the interface area between heat affected zone and weld metal were given in Fig. 10. The results showed that the δ-ferrite content decreased to ~1% when the heat input was about 2.25kJ.
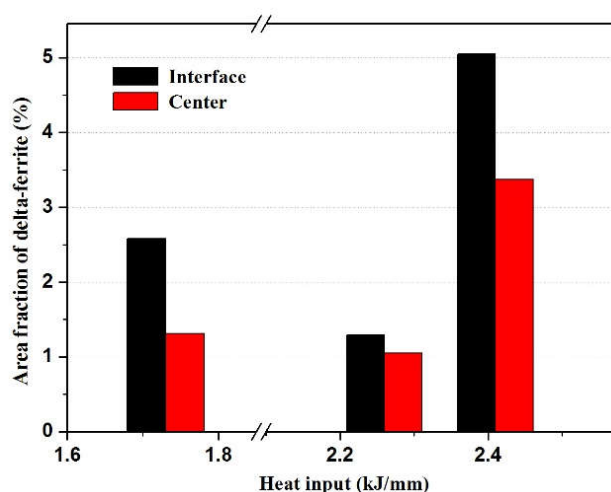

Fig. 10. Area fraction of δ-ferrite under different welding conditions.

The weld stress distribution along the welding direction under conditions of constant fully constrained and fully constrained while welding and removed the clamps after welding were measured. As shown in Fig. 11, the weld stress peak value under constant fully constrained condition was up to 360 MPa, nearly 65% of yield strength of CLAM steel. After removing the clamps, the weld stress especially the stress vertical to the weld line reduced obviously. Even the compression stress horizontal to the weld line was observed at the beginning and end of the weld line. The influence of the weld stress on the microstructure and mechanical properties was being investigated. The systemic research on mechanical properties such as creep and fatigue of the weldments is also planned.
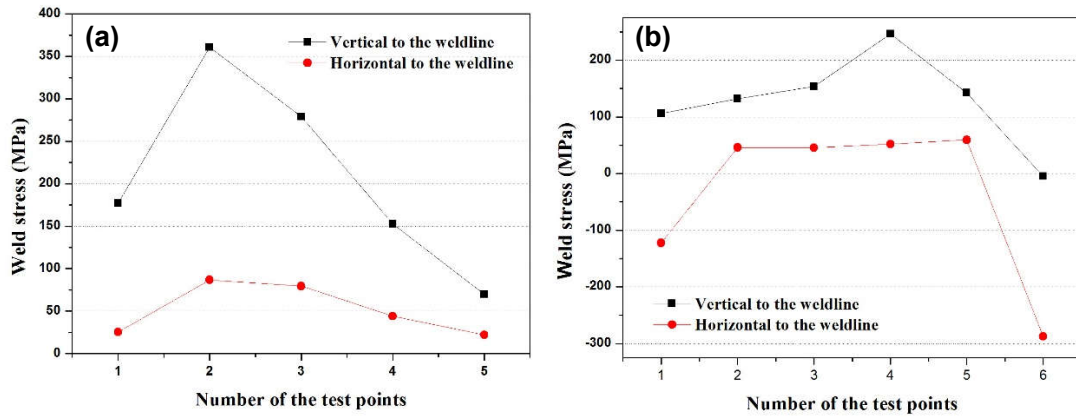
Fig. 11. Weld stress distribution along the welding direction (a) constant fully constrained (b) fully constrained while welding and removed the clamps after welding.

3. Code qualification for ITER-TBM application

Due to the highest priority of safety in nuclear industry, a set of rules for design and construction of nuclear reactors have been set up. These rules are compiled and presented in codebooks such as ASME and RCC-MRx, which include the requirements for material qualification. Depending on the category of the component to be constructed with these materials, the highest requirement will be required for critical components acting as safety barrier to radiation hazards.

ITER-TBMs will demonstrate viability of tritium breeding systems for future demonstration and power reactors. Obviously any failure of these modules not only will undermine future development work but also will affect the ITER operation with potential safety hazards capable of affecting public perception of fusion machines. As a result, one can reasonably assume that the ITER management will not authorize insertion of any ITER TBM whose structural materials are not qualified.

CLAM steel is to be used as the primary structural material for the Chinese TBMs. Just as the Eurofer steel was fully qualified for the European TBMs, CLAM steel has to be qualified for the Chinese TBMs. This is also the case for the Japanese, Indian and the Korean TBM steels. Since 2001, great efforts on the development of CLAM steel have been made. Following the large industrial scale production of F82H and Eurofer97 at more than 10 to 20 tons per heat, CLAM steel has gone through similar scale-up to industrial production practices and reached to 6.4-ton heat. A large number of experimental tests performed have shown that the overall properties (including physical properties, mechanical properties, compatibility with lead-based alloy, compatibility with tritium and neutron irradiation properties etc.) of CLAM steel are very good and the related R&D technology of joint is well developed and well defined for the fabrication of the TBM. The material database of CLAM steel, although yet insufficient, basically meets the requirements of TBM design, which means that it is on the way to meet the code qualification status for China ITER-TBM. As one of the three most well-known RAFMs which have reached the industrial production, CLAM steel is on its way for fully qualification to final successful application in advanced energy systems (such as fusion reactors and lead-based fast reactors etc.) in the near future.

4. Innovative designing theory based on current progress

Current results indicate that RAFM steel fulfills the requirements of ITER, considering its strength, creep properties, irradiation resistance, and application temperature. However, the application

temperature of structure materials can exceed 600 °C to improve the efficiency of fusion power plants, coupled with the neutron irradiation dose up to 200 dpa. A lot of work is needed to further improve the upper application temperature and irradiation resistance of CLAM steel.

4.1 Selective secondary phase strengthening

4.1.1   Thermal stability of precipitates

As known, the upper application temperature of RAFM steel is ~550 °C, its mechanical strength will decrease rapidly at the elevated temperatures. It is expected that the application temperature be improved to over 650 °C or even higher. As the high temperature strength of alloys and steels is highly dependent on the secondary precipitates, thermal stability of precipitates in CLAM steel is one of the major concerns for improving the properties of CLAM steel at elevated temperature.

Several types of secondary phases have been identified in the CLAM steel, such as $M_{23}C_6$, MX, Z phase and Laves phase. MX phase can stand for much higher temperature up to over 1000 °C. Strengthening of CLAM steel by selected precipitates such as TaC is under investigation. There are two methods to improve the phase fraction of TaC in the CLAM steel. First method is to increase the Ta content. However, too much Ta may lead to the decrease of ductility. The effect of Ta content on mechanical properties and ductility is intensively investigated, and a Ta content of 0.18% was chosen for the production of the 6.4 ton CLAM steel, which demonstrated a higher volume fraction of TaC precipitates and better creep properties compared with that of a lower Ta content. The other method is by using optimization of fabrication processes. Thermomechanical treatment (TMT) process is being applied to improve the number density, reduce the precipitate size, and to increase the fraction of MX (TaC and TaN) precipitates in CLAM steel.

4.1.2   Irradiation stability

The stability of precipitates under irradiation is an important factor of high temperature performance for pinning dislocation, martensitic lath boundaries and prior austenitic grain boundaries, etc. However, most ferritic/martensitic steels show obviously weakening at temperatures above 600 °C due to reduced pinning effect of coarsened/dissolved precipitates. Generally, stability of MX-type nano-precipitates, mainly including TaC, TaN, VN, is a key factor to improve high temperature strength of RAFM steel over 600 °C. Hence, the irradiation stability of MX   phase should be paid more attention in developing new RAFM steel. H. Tanigawa et al. have investigated the instability of precipitates in RAFM steel under ion irradiation [24]. It showed that the TaC precipitate would dissolve after irradiation by Fe^{3+} ion, the similar results were observed in the ORNL 9Cr-2WVTa and JLF-1RAFM steel under neutron irradiation up to 5 dpa at 300 °C [25]. L. Tan et al. have done some researches on the stability of MX in ferritic steels under ion irradiation [24, 25]. The results showed that TaC and TaN presented good irradiation stability under a dose of 20 dpa, but the irradiation stability of VN was relatively weak. The VN nanoprecipitates had grown as a rod and presented low number density as shown in Fig. 12 [26], that was different from TaN and TaC. And the N-rich precipitates Ta (C, N) exhibited obviously lower stability than TaC during ion irradiation experiments [27]. Therefore, the amount of TaC should be improved in the next new RAFM steel while limit N-rich precipitates such as VN and Ta (C, N). And the nitrogen content in RAFM steel should be limited for superior performance at high temperature.
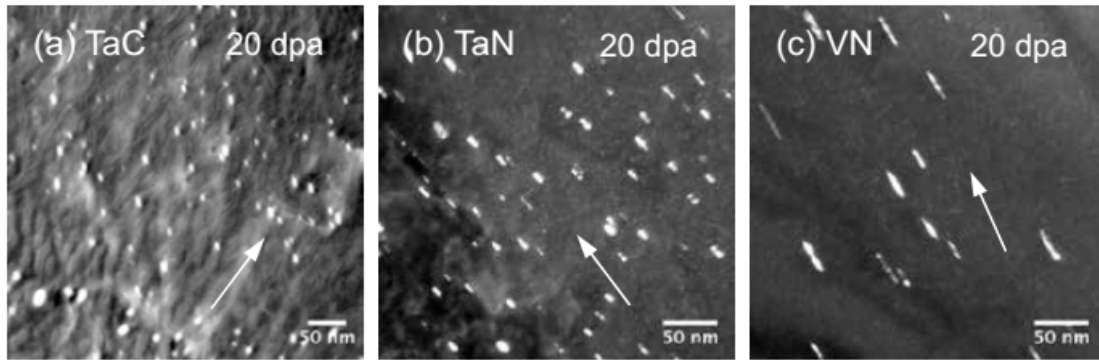
Fig. 12. Morphological characteristics of MX-type nano-precipitates under ion irradiation [25].

4.1.3 New generation irradiation resistant CLAM steel

To improve the high temperature performance of RAFM steels, the oxide dispersion strengthened (ODS) steels with addition of Y_2O_3 particles that based on RAFM steels, such as the ODS-Eurofer97, ODS-F82H, and other 9Cr-ODS steels, have been developed in Europe, Japan and other countries [28-30]. Nano-oxide particles dispersed inside the matrix act as obstacles to the dislocation motion and significantly improve the creep resistance and neutron irradiation resistance [31, 32]. The ODS steels by addition of thermally stable oxide particles could improve the operating temperature to about 650°C or even higher [33]. The oxide dispersion strengthened (ODS) CLAM steel was fabricated by mechanical alloying (MA) and HIP. The microstructural evolutions during the process of ball milling and subsequent consolidating were investigated by SEM, XRD and TEM. Observation on the consolidated and further heat-treated ODS-CLAM steel samples indicated that a ferrite-martensite dual phase microstructure with a high density of nano-particles was achieved, as can be seen in Fig. 13.
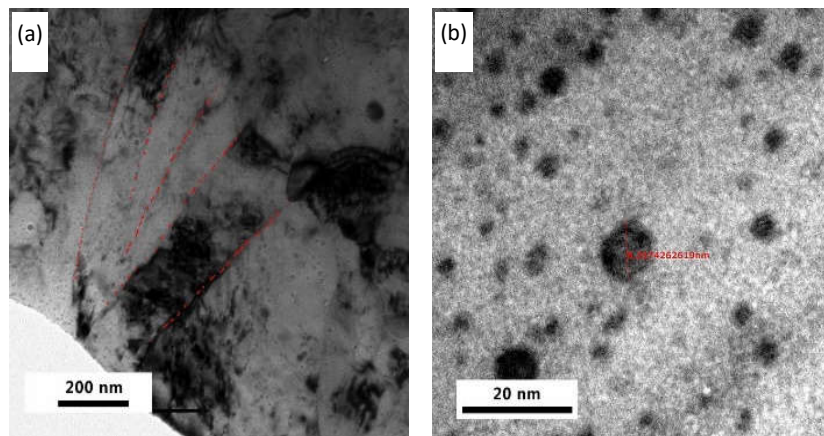

Fig. 13. TEM images of (a) martensitic lath zone and (b) the distribution of the high-density nano-particles in the ODS-CLAM steel.

4.1.4 Components fabricated by additive fabrication

Based on the service environment of the blanket in the fusion reactor, with the high nuclear thermal deposition, the blanket components were usually designed with high density and complex embedded cooling channels, and the fabrication of the blanket components by traditional techniques are facing with great challenges. At present, additive manufacturing offers the potential path that the complex and net-shape parts, as the blanket components of the fusion reactor, can be built feasibly at once.

In our institute, the selective laser melting (SLM) processing, one of the additive manufacturing

methods, was used to investigate the manufacturing techniques of China ITER TBM with CLAM steel powders. The CLAM steel powders, as showed in Fig. 14 (a), were produced by the method of atomization comminuting process, and its particle size with 45–105 μm and a mean particle size of 76 μm as the raw material of SLM processing.
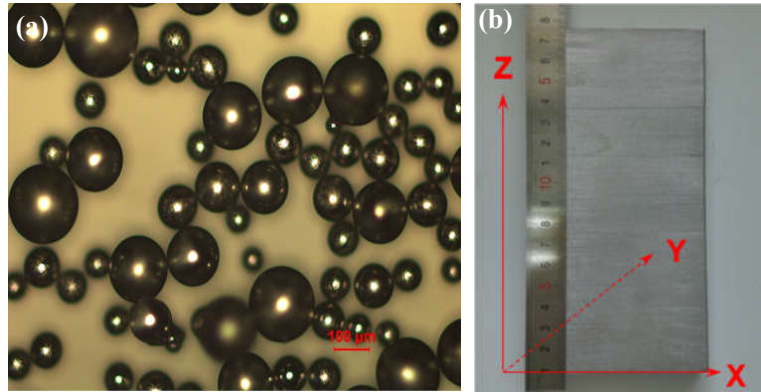

Fig. 14. CLAM steel powders (a) and block prototype fabricated by SLM (b).

The effect of SLM processing parameters on microstructures and mechanical properties were investigated and the suitable SLM processing window was obtained. And a block prototype was fabricated with the size of 100 mm (length)×12 mm (thickness)×170 mm (height), which was showed in Fig. 14 (b). Preliminary measurement, the as-built density was reached 99.7% of the hot-rolled CLAM steel.

The microstructures and mechanical properties were analyzed at the conditions of SLM status, post-SLM heat treatment (HT) status with 740 °C /90 min, the results showed that the microstructures consisted of thin martensitic laths and a small quantity of delta-ferritic, and with the main defects of powders incomplete fusion and micro-cracks as Fig. 15 shown.
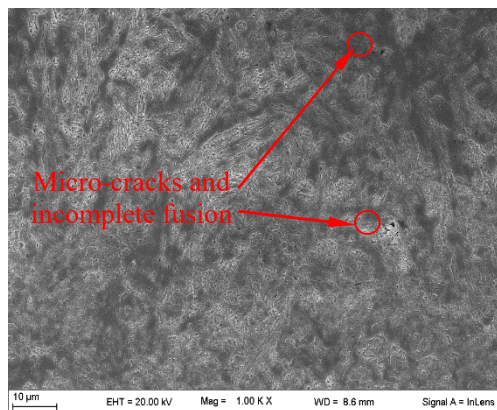

Fig. 15. Microstructure and the main defects of CLAM SLM prototype.

The results of mechanical properties under various states showed that the anisotropic mechanical properties was obvious at SLM status and SLM post-HT status, the properties were mainly performed with brittle and the difference of properties between the layers direction and accumulation direction were only partly reduced by the HT treatment after SLM, the anisotropic mechanical behavior was still serious.

At present, the most important problems might be the stress cracking, due to the complexity structures of components and long-term continuously manufacturing. For solving this problem, the process

improvement and optimization of SLM should be focus researched in the future works.

5. Strategy for further development and application

5.1 Short-term and long-term development priorities

5.1.1 Short-term: joining technology

The full qualification of CALM steel will take several years and for CLAM to be fully qualified in time for construction of Chinese TBM, the whole process must be completed within 2 to 3 years before the actual construction of TBMs and expected insertion in ITER (currently 2019). Furthermore, the code qualification of a new material is an expertise that once obtained for CLAM can be used for future materials in both fission and fusion.

5.1.2 Long-term: CLAM-ODS

ODS version of CLAM steel, nominated as CLAM-ODS, is considered as a variation of CLAM steel developed for higher temperature applications, such as future fusion power plants, as well as Gen. IV fission reactors [34]. Current study shows that CLAM-ODS steel samples with a martensitic matrix and a high number density of nano-sized oxide particles can be fabricated. To realize its industrial application, however, the production scale should be greatly improved. It is thus a major challenge for the development of CLAM-ODS steel. Corresponding research is underway, and the focus is on the innovative fabrication of the CLAM-ODS steel.

6. Summary

Great efforts have been devoted to the research and development of CLAM steel: the fabrication processes were mature; the material properties, including mechanical properties, corrosion, irradiation and joining etc., basically met with the requirement of TBM. CLAM steel has been selected as the unique candidate structural material for CN ITER TBM and the qualification is underway.

Newly fabricated 6.4 tons CLAM steel with a higher Ta content and optimized fabrication processes exhibits high mechanical strength, good creep properties and superior performance over previous heats. It indicates that the controlled precipitation of secondary phases, such as TaC and TaN, can substantially contribute to the improvement of the properties of CLAM steel. The 6.4 ton heat of CLAM steel is strictly tested and analyzed for the database of qualification.

New generation of CLAM steel with higher upper application temperature up to 650 °C and better irradiation resistance is being developed by using TMT processes, as well as nano-oxide dispersion strengthening. It is also expected that CLAM steel may be applied to nuclear parts that require higher application temperature and higher irradiation damage.

Reference

[1] Baluc N., et al., "Status of R&D activities on materials for fusion power reactors", Nucl. Fusion **47** (2007) S696–S717.

[2] Kurtz R.J., et al., "Recent progress toward development of reduced activation ferritic/martensitic steels for fusion structural applications", J. Nucl. Mater. **386–388** (2009) 411–417.

[3] Huang Q.Y., et al., "Status and strategy of fusion materials development in China", J. Nucl. Mater. **386-388** (2009) 400-404.

[4] Huang Q.Y., et al., "Recent progress of R&D activities on reduced activation ferritic/martensitic steels", J. Nucl. Mater. **442** (2013) S2-S8.

[5] Huang Q.Y., et al., "Progress in development of China low activation martensitic steel for fusion application", J. Nucl. Mater. **367-370** (2007) 142-146.

[6] Huang Q.Y., et al., "Progress in development of CLAM steel and fabrication of small TBM in China", J. Nucl. Mater. **417** (2011) 85-88.

[7] Huang Q.Y., "Development Status of CLAM Steel for Fusion Application", J. Nucl. Mater. **445** (2014) 649-654.

[8] Wu Y.C., "Fusion-based hydrogen production reactor and its material selection", J. Nucl. Mater. **386** (2009) 122-126.

[9] Wu Y.C., "Design status and development strategy of China liquid lithium-lead blankets and related material technology", J. Nucl. Mater. **367-370** (2007) 1410-1415.

[10] Huang Q.Y., et al., "Latest progress on R&D of ITER DFLL-TBM in China", Fusion Eng. Des. **86** (2011) 2611-2615.

[11] Liu S.J., et al., "Influence of non-metal inclusions on mechanical properties of CLAM steel", Fusion Eng. Des. **84** (2009) 1214-1218.

[12] Li Y.F., et al., "Mechanical Properties and Microstructures of China Low Activation Martensitic Steel Compared with JLF-1", J. Nucl. Mater. **367-370** (2007) 117-121.

[13] Gao S., et al., "Corrosion behavior of CLAM steel in static and flowing LiPb at 480 °C and 550 °C", Fusion Eng. Des. **86** (2011) 2627-2631.

[14] Peng L., et al., "Microstructure and microhardness of CLAM steel irradiated up to 20.8 dpa in STIP-V", J. Nucl. Mater. **468** (2016) 255-259.

[15] Huang Q.Y., et al., "Study of Irradiation Effects in China Low Activation Martensitic Steel", J. Nucl. Mater. **329** (2004) 268-272.

[16] Zhang J.Y., et al., "Overview on the welding technologies of CLAM steel and the DFLL TBM fabrication", Nucl. Mater. & Energy, http://dx.doi.org/10.1016/j.nme.2016.03.003.

[17] Tavassoli A. -A., et al., "Materials design data for reduced activation martensitic steel type F82H", Fusion Eng. Des. **61** (2002) 617-628.

[18] Zhai X.W., et al., "Effect of tantalum content on microstructure and tensile properties of CLAM steel", Fusion Eng. Des. **104** (2016)21-27.

[19] Zhao Y.Y., et al., "Low cycle fatigue properties of CLAM steel at 450 °C and 550 °C", Fusion Eng. Des. **112** (2016)213-217.

[20] Sandor B.I., Fundamentals of cyclic stress and strain, Univ of Wisconsin Pr, 1972.

[21] Pramanik B., et al., "Surface fractal analysis for estimating the fracture energy absorption of nanoparticle reinforced composites", Materials, **5** (2012) 922-936.

[22] Zhong B., et al., "Creep deformation and rupture behavior of CLAM steel at 823 K and 873 K", J.

Nucl. Mater. **455** (1–3) (2014) 640–644.

[23] Hu X., et al., "Evolution of microstructure and changes of mechanical properties of CLAM steel after long-term aging", Mater. Sci. Engin.: A **586** (2013) 253-258.

[24] Tanigawa H., et al., "Radiation induced phase instability of precipitates in reduced-activation ferritic/martensitic steels", J. Nucl. Mater. **367-370** (2007) 132-136.

[25] Tanigawa H., et al., "Microstructure property analysis of HFIR-irradiated reduced-activation ferritic/martensitic steels", J. Nucl. Mater. **329-333** (2004) 283-288.

[26] Tan L., et al., "Stability of the strengthening nanoprecipitates in reduced activation ferritic steels under Fe2+ ion irradiation", J. Nucl. Mater. **445** (2014) 104-110.

[27] Tan L., et al., "Stability of MX-type strengthening nanoprecipitates in ferritic steels under thermal aging, stress and ion irradiation", Acta Materialia **71** (2014) 11-19.

[28] Lindau R., et al., "Present development status of EUROFER and ODS-EUROFER for application in blanket concepts", Fusion Eng. Des., **75-79** (2005) 989-996.

[29] Lindau R., et al., "Mechanical and microstructural properties of a hipped RAFM ODS-steel", J. Nucl. Mater. **307** (2002) 769-772.

[30] Wu X., et al., "The microstructure characterization of reduced activation F82H-ODS ferritic steel", J. Nucl. Mater. **452** (2014) 212–217.

[31] Brocq M., et al., "Nanoscale characterization and formation mechanism of nanoclusters in an ODS steel elaborated by reactive-inspired ball-milling and annealing", J. Nucl. Mater. **409** (2011) 80-85.

[32] Lucon E., et al., "Mechanical response of oxide dispersion strengthened (ODS) EUROFER97 after neutron irradiation at 300°C", Fusion Eng. Des., **82** (2007) 2438-2443.

[33] Revol S., et al., "Development of the elaboration process and joining technologies of RAFM ODS steels", Fusion Eng. Des., **58-59** (2001) 761-765.

[34] Ukai S., et al., "Production and properties of nano-scale oxide dispersion strengthened (ODS) 9Cr martensitic steel claddings", ISIJ Int. **43** (2003) 2038-2045.